

# *METABOLIC AND OSTEOGENIC SUSCEPTIBILITY IN DISH: A PROGNOSTIC INDEX FROM PROPENSITY SCORE MODELLING*

---

*E Pariente, M Martín-Millán, M Maamar, J Pardo-Lledías, H Basterrechea, B Petitta, C Bianconi,  
C Ramos-Barrón, V Martínez-Taboada, JL Hernández*

## **\* Correspondence to:**

Emilio Pariente (MD, PhD)

“Camargo Interior” Health Care Center

Associate Professor, Department of Medicine and Psychiatry, University of Cantabria

Avda Bilbao, s/n. 39600-Muriedas, Cantabria, Spain

Tel: +34 942 254 499

Email: [emilio.pariente@scsalud.es](mailto:emilio.pariente@scsalud.es)

ORCID id: 0000-0003-0035-3298

**Accepted Manuscript (Author Accepted Version)** of the article:

*"Metabolic and osteogenic susceptibility in DISH: A prognostic index from propensity score modelling"*

*The final Version of Record is published in Bone (Elsevier).*

DOI: <https://doi.org/10.1016/j.bone.2026.117819>

© 2026 Elsevier. This work is licensed under [CC BY-NC-ND 4.0](https://creativecommons.org/licenses/by-nc-nd/4.0/)

## AUTHORS

### Filiation and contribution

Emilio Pariente (1,2,3) ORCID id: <b>0000-0003-0035-3298</b>	emilio.pariante@scsalud.es	Conceptualization Investigation Methodology Writing—original draft
Marta Martín-Millán (2,3,4)	marta.martinm@scsalud.es	Investigation Writing—original draft
Meryam Maamar (5)	meryyop92@gmail.com	Data curation Writing—original draft
Javier Pardo-Lledías (2,3,4)	javier.pardo@scsalud.es	Investigation Data curation
Héctor Basterrechea (6)	hectorbas.hb@gmail.com	Investigation Data curation Visualization
Benedetta Petitta (1)	benedetta.petitta@gmail.com	Data curation Visualization
Camila Bianconi (1)	cmlb12@hotmail.com	Investigation Data curation
Carmen Ramos-Barrón (2,3,7)	carmen.ramos@unican.es	Methodology Validation
Víctor Martínez-Taboada (2,3,8) ORCID id: <b>0000-0003-2916-8491</b>	victormanuel.martinez@scsalud.es	Methodology Supervision Reviewing and editing
José Luis Hernández (2,3,4) ORCID id: <b>0000-0002-6585-8847</b>	hernandezjluis@gmail.com	Conceptualization Methodology Supervision Reviewing and editing

1 Healthcare Center Camargo-Interior, Cantabrian Health Service, Santander, Spain;

2 Department of Medicine and Psychiatry, University of Cantabria, Santander, Spain;

3 Immunopathology Research Unit, Instituto de Investigación Valdecilla (IDIVAL), Santander, Spain;

4 Bone Metabolism Unit, Department of Internal Medicine, Hospital Marqués de Valdecilla, Santander, Spain;

5 Osakidetza Emergency Department. Bilbao, Spain

6 Healthcare Center Gama, Cantabrian Health Service, Santander, Spain;

7 Healthcare Center Camargo-Costa, Cantabrian Health Service, Santander, Spain;

8 Division of Rheumatology, Hospital Marqués de Valdecilla, Santander, Spain

All authors have read and have reviewed and approved the submitted version of the manuscript.

## **ETHICS**

The tenets of the Declaration of Helsinki in research on human subjects were followed. All patients who met the inclusion criteria were informed of the purpose of the study with an informative sheet and were invited to participate. There was no refusal to participate. The study has been conducted according to all relevant national regulations and institutional policies and has been approved by the Regional Ethics Committee (CEIm Internal Code: 2018.188).

## **DECLARATION OF FUNDING**

This research has been supported by a grant from Instituto de Salud Carlos III (PI21/00532) co-funded by European Union FEDER funds.

## **DECLARATION OF FINANCIAL/OTHER RELATIONSHIPS**

The authors have no relevant affiliations or financial involvement with any organization or entity with a financial interest in or financial conflict with the subject matter or materials discussed in the manuscript. This includes employment, consultancies, honoraria, stock ownership or options, expert testimony, grants or patents received or pending, or royalties.

## **DATA SHARING**

The data that support the findings of this study are available from the corresponding author upon reasonable request.

## **ACKNOWLEDGEMENTS**

The authors would like to thank OpenAI's ChatGPT for its support with manuscript refinement. They would also like to thank the study participants and the entire Camargo Cohort group.

## ABSTRACT

### Objective

Diffuse idiopathic skeletal hyperostosis (DISH) is increasingly recognised as a systemic condition associated with trabecular deterioration, and metabolic or vascular disruption. Within this spectrum, a phenotype characterised by accelerated skeletal progression has been described (Fast Ossifier, FO). We aimed to develop sex-specific prognostic indices derived from propensity score (PS) covariates —FOSSI-F (women) and FOSSI-M (men)—to stratify the risk of FO status within a population-based cohort.

### Methods

Using longitudinal data from the Camargo Cohort, sex-stratified logistic models were constructed based on PS-derived upstream variables. Internal validation (bootstrap), discriminative performance (ROC/AUC) and exploratory analyses (non-linear models, clustering, Shapley- $R^2$  decomposition) were performed,

### Results

We analysed 178 individuals (61 with FO; 64% women; mean age=61  $\pm$  7 years). FOSSI-F included visceral adiposity and hypertension, FOSSI-M included waist circumference, and both incorporated age, body mass index and cardiometabolic index. They showed high discriminatory capacity (AUC=0.875 in women and 0.836 in men). Non-linear modelling revealed a broad sigmoid transition zone in women (approximately 5.8–9.6) and a sharp threshold-like pattern in men (0.45–0.71). In high FOSSI values, clustering analyses identified insulin resistance predominating in women and endocrine–inflammatory signals in men. Shapley analysis revealed TyG as the most influential factor in FOSSI-F variance (79.8%), while iPTH was in FOSSI-M (59.5%). Both indices correlated inversely with trabecular bone score ( $p < 0.0001$ ).

### Conclusion

FOSSI-F and FOSSI-M are sex-specific, PS-derived prognostic indices that capture latent metabolic–osteogenic susceptibility associated with FO status. Their strong internal discrimination supports their use for risk stratification and research-oriented interpretation.

### KEYWORDS:

Diffuse idiopathic skeletal hyperostosis; Fast ossifier; Sex differences; Propensity score; Prognostic tool

## RESEARCH IN CONTEXT

**Evidence before this study:** *DISH is a systemic condition with heterogeneous progression. The 'Fast Ossifier' (FO) phenotype denotes rapid ossification, but no tools existed to stratify this risk prospectively.*

**Added value of this study:** *We derived and internally validated one of the first sex-specific prognostic indices (FOSSI-F, FOSSI-M) from propensity score modelling. They show high discrimination, reveal distinct sex-specific metabolic/endocrine pathways, and estimate intervention windows.*

**Implications of all the available evidence:** *FOSSI provides a framework for early risk assessment in DISH, enabling targeted monitoring and research. It exemplifies how causal inference methods can be translated into biologically coherent prognostic tools.*

*METABOLIC AND OSTEOGENIC SUSCEPTIBILITY IN DISH:  
A PROGNOSTIC INDEX FROM PROPENSITY SCORE MODELLING*

## **1. INTRODUCTION**

Diffuse idiopathic skeletal hyperostosis (DISH) is characterised by flowing ossification of the anterior longitudinal ligament and widespread enthesal hyperostosis. Once regarded as a benign, slowly progressive condition of ageing, and largely limited to ligamentous ossification, accumulating evidence now challenges this view. DISH is increasingly recognised as a systemic osseous disorder marked not only by hyperostosis but also by trabecular deterioration [1], metabolic dysregulation [2], and a heightened risk of cardiovascular disease, including incident ischaemic stroke [3]. Together, these findings call into question the traditional notion of DISH as a purely structural condition.

Recent studies further suggest that skeletal progression in DISH may be faster and more heterogeneous than previously assumed. Younger individuals [4] and those with obesity [5] appear particularly susceptible to accelerated axial ossification, pointing to systemic metabolic factors as potential modulators of disease trajectory. Supporting this heterogeneity, longitudinal data from the Camargo Cohort identified a subset of individuals who developed early and rapid axial ossification with concomitant trabecular decline, the Fast Ossifier (FO) phenotype [6]. Although pending external validation, this phenotype implies that DISH does not follow a uniform progression and that certain individuals may exhibit a markedly higher metabolic–osteogenic susceptibility. This convergence of accelerated ossification, trabecular decline, and metabolic burden underscores the need to detect high-susceptibility individuals. Early identification of such persons could have direct implications for monitoring, risk counselling, and mechanistic research.

Despite these insights, no prognostic framework currently exists for DISH, in stark contrast to other rheumatic diseases, such as rheumatoid arthritis, axial spondyloarthritis, and psoriatic arthritis, where composite indices are integral to risk stratification and management [7–11]. No analogous instrument is available for DISH, despite its systemic complications and growing prevalence. This gap is particularly notable given the emerging recognition of its metabolic and vascular dimensions.

During the development of the propensity score (PS) framework, we observed previously unrecognised associations between PS values and markers of insulin resistance and adiposity, even among individuals without radiographic evidence of DISH. As illustrated in **Suppl Mat, Annex 1**, higher PS values were consistently associated with increasing TyG index tertiles and with FO status. This observation is consistent with prior reports indicating that PS distributions may reflect disease severity, comorbidity burden, and subclinical dysfunction beyond their original role in confounding control [12,13].

Importantly, when the PS was applied for matching, we noted a secondary and informative phenomenon: several metabolic and skeletal variables not explicitly included in the PS model also converged between matched groups, achieving standardised mean differences below conventional thresholds ( $|SMD| < 0.1$ ) (**Suppl Mat, Annex 2**). This finding suggests that the PS was not merely balancing the selected covariates, but was acting as a proxy for a broader, latent metabolic–osteogenic configuration encompassing interconnected biological pathways not directly specified in the model.

These observations support the interpretation of the PS as an indicator of a broader, system-wide pathological state, in which the measured covariates represent only the visible component of a largely submerged biological substrate underlying DISH. In fact, although traditionally used for confounding adjustment, the PS seems to encode latent disease susceptibility when derived from biologically plausible upstream variables [12–14]. In this context, we explored the internal structure of the PS by stratifying individuals according to its distribution and observed that the high-PS group displayed clear sex-specific clustering of clinical and metabolic features (**Suppl Mat, Annex 3**).

Recent methodological advances in causal modelling propose that the PS can function as a prognostic analogue, condensing multidimensional biological information into a parsimonious and interpretable scalar [15]. Collectively, these observations provided a rationale for investigating whether the latent biological signal embedded within the PS could be recalibrated into a meaningful prognostic framework for DISH. The absence of existing tools for risk stratification, the demonstrated heterogeneity in disease trajectories, and the evolving interpretation of PS models converge on a clear unmet need. This convergence supports a theory-driven approach in which the PS is not merely a source of covariates, but a conceptual scaffold for deriving a prognostic index that captures the core metabolic–osteogenic susceptibility underlying DISH progression.

Accordingly, we sought to develop and perform internal validation of two sex-specific indices derived from the PS structure to estimate metabolic–osteogenic susceptibility and stratify risk of accelerated DISH progression. In a condition long considered homogeneous yet increasingly recognised as biologically diverse, this study provides a first framework for structured prognostic differentiation.

## **2. METHODS**

### **2.1 Study design**

Using longitudinal data from the Camargo Cohort, the aim was to develop two sex-specific indices for stratifying the risk of accelerated progression in DISH: Fast Ossifier Stratification Index (FOSSI), that comprises FOSSI-F for women and FOSSI-M for men. The Camargo Cohort is a longitudinal, population-based study initiated in 2006 and conducted in Northern Spain to investigate the incidence and progression of metabolic bone diseases in postmenopausal women and men aged  $\geq 50$  years. It integrates anthropometric, metabolic, radiographic, and clinical assessments collected at baseline and at 5-year intervals. Detailed cohort methodology has been previously published [16].

### **2.2 Radiological Assessment and 'Fast Ossifier' definition**

DISH was diagnosed according to the radiographic criteria proposed by Resnick and Niwayama, which require the presence of flowing ossifications along the anterolateral aspect of at least four contiguous vertebral bodies of the thoracic spine, preservation of intervertebral disc height without extensive degenerative disc disease, and absence of apophyseal joint ankylosis or sacroiliac joint erosion, sclerosis, or fusion.

The Schlapbach Graded Scale is a semi-quantitative tool routinely used in this cohort to characterise changes related to DISH on plain radiographs [17]. It includes four grades ranging from grade 0 (no ossification) to grade III, which coincides with the diagnostic criterion proposed by Resnick and Niwayama (**Figure 1**). A previous study by our group focused on the reliability of this scale yielded weighted kappa values greater than 0.80 for both intra- and interobserver agreement [18]. After receiving training from a senior radiologist, two investigators from the cohort performed the evaluation independently and blinded to the clinical data.

Fast Ossifier (FO) status was defined a priori as progression of  $\geq 2$  Schlapbach grades between two consecutive cohort assessments and was analysed as a transversal phenotype reflecting accelerated biological activation rather than cumulative disease burden [6]. This definition was chosen to specifically capture dynamic progression over time, independently of baseline radiographic severity. This distinction allowed us to differentiate accelerated progression from established structural disease and to focus the prognostic modelling on individuals at risk of rapid skeletal or metabolic-vascular disruption.

## **2.3 Conceptual Framework and Derivation of the Fast Ossifier Stratification Index (FOSSI)**

### **2.3.1. Upstream Susceptibility vs. Downstream Activation**

From a causal perspective, we distinguished between 'upstream' and 'downstream' factors in the pathobiology of DISH. Upstream factors constitute a relatively stable biological background that precedes and permits pathological activation. The variables selected for the original PS model -age, sex, obesity, type 2 diabetes (T2DM), hypertension, waist circumference (WC), and metabolic syndrome (MetS)- are archetypal upstream factors. They are temporally stable, precede overt skeletal changes, and collectively define a state of latent metabolic-osteogenic susceptibility.

In contrast, downstream regulators are dynamic biomarkers of active pathophysiological processes. In line with the characterisation of the FO phenotype [6], we focused on three key downstream regulators: insulin resistance (assessed by the Triglyceride-Glucose index, TyG), systemic inflammation (evaluated by the Albumin-to-Globulin Ratio, AGR), and endocrine-mineral balance (intact parathyroid hormone, iPTH). These markers reflect active metabolic, inflammatory, and endocrine dysregulation directly implicated in accelerated ossification.

This conceptual distinction is central to our study design. FOSSI was constructed exclusively from upstream susceptibility factors to capture baseline risk. The potent downstream regulators (TyG, AGR, iPTH) were intentionally excluded from the final index equations to preserve FOSSI's role as a measure of latent susceptibility, rather than an exclusively marker of concurrent biological activation.



Thus, FOSSI captures latent susceptibility that precedes—and anticipates—downstream biological activation, without directly incorporating activation markers into the index.

### **2.3.2. Analytical Pathway: From Susceptibility Profiling to Progression Modelling**

The development of FOSSI proceeded in three sequential steps designed to isolate the signal for rapid progression within a context of high baseline susceptibility.

**Phase 1:** Identification of a High-Susceptibility Cohort. All individuals with DISH in the Camargo Cohort were matched to non-DISH controls using a PS model based on the upstream factors listed above. This generated a group of controls sharing a high underlying susceptibility profile with the DISH cases. From this pool, participants in the highest PS tertile were selected for longitudinal follow-up.

**Phase 2:** Longitudinal Phenotyping and Cohort Balancing. During follow-up, 61 participants developed the Fast Ossifier (FO) phenotype. These individuals, together with 117 PS-matched controls from the same high-susceptibility pool who did not progress (Non-Progressors, NP), formed the analytical sample. Balance diagnostics (standardized mean differences, variance ratios, McFadden's pseudo- $R^2$ ; **Suppl Mat, Annex 4**) confirmed that the high covariate balance achieved by the initial PS matching was preserved between the FO and NP groups. This ensured both groups shared an equivalent baseline metabolic and anthropometric profile, making the sample methodologically appropriate for modelling progression risk independent of baseline susceptibility.

**Phase 3:** Derivation of the Sex-Specific FOSSI Indices. Within this balanced FO/NP cohort, FO status was used as the binary dependent variable. The upstream PS components served as candidate predictors. To preserve biological coherence and avoid data-driven overfitting, the construction of FOSSI was intentionally restricted to these covariates. Sex-specific logistic regression models were fitted. Univariate analyses assessed associations with FO status, followed by multivariable modelling where variance inflation factors (VIF) identified and addressed collinearity. Variables with minimal predictive power or high redundancy were removed. This process yielded the final, parsimonious equations for FOSSI-F and FOSSI-M.

In summary, the PS model identified the shared metabolic profile of susceptibility to DISH. By refitting its upstream components within a longitudinally derived, balanced cohort of

individuals who all share this high-risk profile, FOSSI isolates the specific metabolic signature that further discriminates rapid progression (FO) from slow progression (NP). Therefore, FOSSI is not a model for the development of DISH, but a prognostic model for the risk of rapid progression *within* DISH.

## 2.4 FOSSI internal validation

While the predictive performance of FOSSI-F and FOSSI-M was evaluated using several complementary approaches, internal validation was based on bootstrapping with resampling. Robustness was examined via bootstrap validation with 1000 resamples, from which median AUC values and 95% confidence intervals were obtained. Additional internal validation included subgroup analyses stratified by age, metabolic profile, presence of metabolic syndrome, and diabetes status. Threshold stability was assessed by perturbing cut-offs by  $\pm 10\%$  and quantifying the resulting changes in accuracy indices [19].

Discrimination was assessed through receiver operating characteristic (ROC) analysis and optimal cut-offs were defined using the Youden index. Sensitivity, specificity, positive predictive value (PPV), and negative predictive value (NPV) were calculated at these thresholds. To characterise potential non-linear associations between FOSSI values and FO status, sex-specific generalized additive models (GAMs) were fitted using age, Triglyceride Glucose (TyG) index, and intact parathyroid hormone (iPTH) as smooth terms. FOSSI values were analysed under two complementary projections: a probabilistic mapping onto FO status and a continuous activation-based representation reflecting downstream phenotypic transformation. Multivariable analyses were then performed to evaluate the association between FOSSI and FO status after adjusting for demographic and clinical covariates. Finally, Shapley decomposition was applied to quantify the relative contribution of each predictor to the explained variance ( $R^2$ ) [20], enabling identification of the dominant biological drivers within each sex.

## 2.5 Statistics

All analyses were performed using SPSS v29 (IBM Corp., Armonk, NY). Shapley- $R^2$  decomposition analyses were performed using the SPSS extension 'Stats Relimp'. Missing data were handled using multiple imputation with regression-based procedures, generating five imputations that were pooled according to Rubin's rules.

Comparability between FO subjects and Non-progressors was analyzed using Python scripts available at <https://zenodo.org/records/15030430>. All statistical procedures followed prespecified analytical protocols. A significance threshold of  $p < 0.05$  was applied, with Bonferroni correction used for multiple comparisons where appropriate.

### 3. RESULTS

#### 3.1 Overall sample

In the overall sample (178 individuals; 64% women, mean age  $61 \pm 7$  years), TyG index, a surrogate marker of insulin resistance, was  $8.48 \pm 0.5$ , and the albumin-to-globulin ratio (AGR) as a marker of inflammation, was  $1.67 \pm 0.3$ . A total of 61 individuals developed the FO phenotype (30 women, 31 men; 18% aged  $<60$  years), and 117 did not progress. Within the FO group, women were younger than men ( $63 \pm 5$  vs.  $69 \pm 8$  years;  $p = 0.0001$ ) and had lower waist circumference (WC), metabolic syndrome (MetS) prevalence, and Charlson comorbidity index. No sex differences were observed in AGR or TyG index.

#### 3.2 FOSSI-F and FOSSI-M: equations and distributions

FOSSI-F incorporated age, body mass index (BMI), cardiometabolic index (CMI), hypertension status, and visceral adiposity index (VAI), according to the following equation:

$$\text{FOSSI-F} = -18.811 + (0.209 \times \text{age}) + (0.350 \times \text{BMI}) + (1.359 \times \text{CMI}) + (0.799 \times \text{hypertension}) + (0.203 \times \text{VAI}).$$
 Among FO cases, FOSSI-F values ranged from 2.65 to 16.31 (median 7.88; IQR 5.85–9.58).

FOSSI-M included age, BMI, CMI, and waist circumference (WC): 
$$\text{FOSSI-M} = -4.663 + (0.039 \times \text{age}) + (0.045 \times \text{BMI}) - (0.223 \times \text{CMI}) + (0.015 \times \text{WC}).$$
 FOSSI-M values ranged from 0.51 to 1.54 (median 0.81; IQR 0.70–1.07).

The distribution of FOSSI-F showed a graded, four-stratum pattern (low, intermediate, high, and very high probability), reflecting progressively increasing within-cohort FO probability across score ranges. By contrast, FOSSI-M exhibited a narrow, threshold-like distribution, with FO cases clustering in FOSSI-M values  $\geq 0.71$ . **Table 1** summarises the characteristics of both indices, including score ranges and corresponding within-cohort probability strata for FO status.

### 3.3 Validation and Exploratory Analyses

The validation and interpretation of FOSSI proceeded in two complementary phases: first, assessment of its prognostic performance and stability (ROC/AUC, Bootstrapping); second, exploration of its biological properties and non-linear relationships with the FO phenotype (GAM for shape, Shapley for drivers, Clustering for construct validity).

#### 3.3.1 Discrimination and Performance

FOSSI-F achieved an AUC of 0.875 (95% CI 0.77–0.97), increasing to 0.913 (95% CI 0.69–0.95) among women <66 years (**Table 2**). At the primary threshold, sensitivity was 83.3% and specificity 78.3% (NPV = 88.5%). Higher cut-offs increased specificity (up to 93.6% at  $\geq 9.58$ ) with lower sensitivity.

FOSSI-M achieved an AUC of 0.836 (95% CI 0.75–0.91), with 81.8% sensitivity and 73.2% specificity, increasing to 0.857 (95% CI 0.76 - 0.95) in men <66 years. Values  $\geq 0.79$  yielded specificity of 91.7%.

#### 3.3.2 Internal Validation and Robustness

Sensitivity analyses supported the robustness of both sex-specific indices. We conducted a comprehensive sensitivity analysis framework consisting of two principal strands: (i) A stability assessment via bootstrapping and (ii) Robustness testing to methodological and definitional variations (including alternative FO definitions and subgroup analysis).

In women, bootstrap resampling yielded discrimination estimates consistent with the primary analysis, indicating stable performance of FOSSI-F across resamples. In men, resampling analyses confirmed the sharp separation between FO and non-FO cases, in line with the near-binary distribution observed in the Non-linear analysis. Given the abrupt risk transition and the potential for overfitting in the male model, a 10-fold cross-validation was performed for FOSSI-M, yielding a mean AUC of  $0.82 \pm 0.04$ . This approach, recommended as a robust measure of out-of-sample predictive performance [21], confirmed that the model had an adequate out-of-sample discrimination and retained high discrimination when evaluated on unseen data. Subgroup analyses demonstrated stable performance across age strata and metabolic subgroups. Perturbation of high-specificity cut-offs ( $\geq 0.79$  for FOSSI-M and  $\geq 9.58$  for FOSSI-F) by  $\pm 10\%$  resulted in minimal loss of specificity ( $>95\%$ ), supporting their use as rule-in thresholds in clinical stratification.

### 3.3.3 Clustering (Construct Validity)

The internal consistency was tested by analysing the most prevalent clusters within the highest FOSSI distribution ranges. Both indices concentrated FO cases, especially those >66 years, in their respective highest range of values (80% of FO females showed FOSSI-F > 7.97, while 89.5% of FO males had a FOSSI-M value > 0.68). They also displayed strong correlations with PS, WC and BMI, and correlated inversely with trabecular bone score (TBS) (**Table 3**). FOSSI-F correlated with metabolic markers of insulin resistance —TyG, Cardiometabolic index (CMI), Visceral adiposity index (VAI)— and inversely with bone-turnover markers (P1NP and CTX). This clustering demonstrated strong construct validity, confirming that individuals with extreme outcome (FO) consistently received extreme scores on the independent risk index (FOSSI)

As shown in **Table 4**, FOSSI-M was primarily associated with inflammatory and endocrine patterns, including low AGR and elevated CTX, alkaline phosphatase, and iPTH. Among FO+ men, those with prior stroke had higher iPTH and alkaline phosphatase levels than those without stroke. No between-group differences were observed in TyG, AGR, total cholesterol, or abdominal aortic calcification score (AAC-24).

### 3.3.4 Exploration of non-linear relationships and biological activation

The non-linear analysis between FO status and FOSSI was used as an advanced performance and exploratory analysis, not as a method of internal validation for model stability. To visualize the continuum of metabolic–osteogenic activation captured by FOSSI, sex-specific GAM were used to project FOSSI scores along two complementary dimensions: the model-based probability of FO status (expressed as expected prevalence) and a normalized index of biological activation toward the FO phenotype (expressed as the range 0–1) (**Figure 2**)

In women, FOSSI-F exhibited a gradual sigmoidal transition (**Fig. 2A**). FO probability remained low (<20%) for scores below 5.84, increased through an intermediate risk zone (5.84–7.88), and exceeded 90% above 9.58. The corresponding normalized activation curve (**Fig. 2B**) rose steadily across this range, indicating that a substantial portion of the downstream osteogenic transformation could be completed even before crossing the high-probability threshold. For example, a FOSSI-F value of 9.12 corresponded to a 75% probability of FO and a normalized activation level of 0.65–0.70, reflecting advanced biological progression.

In men, FOSSI-M displayed a sharp, near-binary transition (**Fig. 2C**). FO prevalence remained low (~12%) until a critical threshold near 0.45, after which it increased steeply, approaching a model-estimated probability of 1.0 when  $\geq 0.71$ . The normalized activation curve (**Fig. 2D**) was similarly abrupt: values below 0.45 reflected minimal activation, whereas values above this threshold indicated rapid progression toward the FO phenotype. A FOSSI-M score of 0.56, for instance, was associated with only 20–25% FO probability but marked the onset of measurable biological activation.

Age-at-threshold (AAT) estimates were derived from the probability-based projections to quantify the temporal dynamics of FO probability. For FOSSI-M, AAT values corresponding to predicted FO probabilities of 20%, 50%, and 80% were 57.0, 58.9, and 60.4 years, respectively, yielding an intervention-window index (IWI) of 3.4 years ( $AAT_{80\%} - AAT_{20\%}$ ). In women, the corresponding AAT values for FOSSI-F were 59.8, 63.8, and 68.1 years, resulting in a substantially wider IWI of 8.3 years.

### 3.3.5 Exploration of biological drivers

Shapley  $R^2$  decomposition identified TyG as the dominant contributor to variance in FOSSI-F (79.8%), while iPTH contributed most strongly to FOSSI-M (59.5%).

ANCOVA confirmed higher FOSSI-F and FOSSI-M values in FO individuals after adjustment (**Suppl Mat, Annex 5**). In logistic regression, FOSSI-F remained independently associated with FO status (adjusted OR = 2.50; 95% CI 1.4–4.2;  $p = 0.001$ ).

## 4. DISCUSSION

### 4.1 Overview

Building on the recently characterised Fast Ossifier (FO) phenotype, this study addresses the need for tools capable of estimating the risk of acquiring FO status at early stages. We developed two sex-specific indices, FOSSI-F and FOSSI-M, designed to quantify metabolic–osteogenic susceptibility using readily available clinical variables.

FOSSI can be conceptualised within a triaxial biological space defined by age, metabolic load, and downstream osteo-endocrine activation (**Figure 3**). Within this framework, individuals may exhibit comparable latent susceptibility while diverging in clinical

expression depending on whether downstream biological vectors become effectively engaged.

The iceberg representation further highlights this distinction. While the FO phenotype constitutes the clinically visible outcome, a larger proportion of the biological process remains subclinical, encompassing metabolic, endocrine, and inflammatory components.

From this perspective, FOSSI fulfils a dual role within the proposed framework: (i) By design, it captures latent metabolic–osteogenic susceptibility, as it is derived exclusively from upstream traits that precede biological activation and define baseline risk. (ii) At the same time, FOSSI operates as a dynamic sensor of downstream activation -the propensity to ossification- with higher values consistently aligning with the engagement of effector pathways and signalling when susceptibility is translated into accelerated ossification. Crucially, this sensing function does not depend on the direct inclusion of activation markers, but on the capacity of FOSSI to anticipate and reflect the biological tension preceding phenotypic transition.

#### **4.2 Biological clustering**

With respect to FOSSI-F and FOSSI-M, BMI and WC emerge as strong upstream correlates, displaying stable associations across both age strata. Interestingly, the PS follows a similar correlation pattern, supporting its interpretation as a composite reflection of underlying cardiometabolic traits rather than an independent downstream construct. Despite their connection to a common metabolic trait represented by BMI and WC, they each captured a distinct sex-specific biological signature.

In women, the highest tertile of FOSSI-F was characterised by an elevated TyG index, visceral adiposity, high CMI, and the frequent use of insulin, oral antidiabetics and statins. In this upper tier, FO status (100%), degraded trabecular bone score (63.8%), high CMI (60%) and ischaemic heart disease (56.3%) were common. This pattern is consistent with insulin resistance-driven susceptibility, a mechanism that has been strongly implicated in metabolic alterations in postmenopausal women [\[22,23\]](#). This aligns with the inverse correlations observed between FOSSI-F and bone turnover markers.

Conversely, FOSSI-M aligned with inflammatory–endocrine pathways. High FOSSI-M values were associated with low AGR, elevated alkaline phosphatase, and high CTX. The most significant clusters in the upper tertile included FO status (100%), anticoagulant use (65%), heart failure (60%), and stroke (52.2%). Although the associations between FO

status, iPTH, alkaline phosphatase, and prevalent stroke derive from small samples and cannot be interpreted as definitive clinical findings, they are compatible with mechanisms implicated in mineral–vascular imbalance and medial arterial calcification [24].

Two findings speak to the internal consistency and construct validity of our approach. First, the clustering of confirmed FO cases in the upper zones of their respective FOSSI scores, and second, the significantly higher FOSSI scores of FO individuals compared to controls, once confounders were controlled for. These findings demonstrate that the empirically defined 'fast ossifier' outcome (based on longitudinal radiography) is robustly linked to its hypothesised metabolic risk profile baseline (quantified by FOSSI). The convergence of these two independent measures — the extreme outcome and the extreme risk score — strongly supports the existence of a distinct metabolic-osteogenic susceptibility phenotype, which is a central premise of our study.

Among key regulators, distinct patterns emerged: insulin resistance dominated FOSSI-F, AGR influenced FOSSI-M, and iPTH contributed to both. Declines in trabecular bone score were evident in women and men alike, consistent with the known detrimental effects of insulin resistance and inflammation on trabecular microarchitecture [25,26]. Thus, FOSSI not only stratifies the risk of accelerated ossification but also reflects underlying trabecular fragility, enhancing its clinical relevance.

### **4.3 Upstream and susceptibility-related covariates**

FOSSI was constructed exclusively from covariates that are relatively stable over time, precede accelerated ossification in the causal sequence, and collectively define a state of latent metabolic–osteogenic susceptibility. This design principle underlies both the inclusion of the cardiometabolic index (CMI) and the visceral adiposity index (VAI), and the deliberate exclusion of potent biological regulators such as TyG index, iPTH, and AGR.

CMI and VAI were retained because they capture early disturbances in lipid metabolism and fat distribution that are known to precede overt insulin resistance and systemic inflammation. By integrating anthropometric and lipid parameters (WC, TG, and HDL cholesterol), these indices reflect a chronic, permissive metabolic environment conducive to accelerated ossification [27]. Their inclusion is consistent with the PS-score architecture from which FOSSI was derived, ensuring that the index represents a composite of predisposing cardiometabolic traits rather than markers of established metabolic dysregulation.



By contrast, TyG, iPTH, and AGR—despite their strong associations with FO status and high explanatory weight in Shapley analyses—were intentionally excluded from the FOSSI equations. These variables operate further downstream in the pathophysiological cascade: TyG reflects insulin resistance with established glycaemic disturbance [28]; iPTH represents endocrine adaptation to mineral imbalance and inflammatory signalling; and AGR captures concurrent systemic inflammation and nutritional status. Incorporating these markers would have transformed FOSSI from a susceptibility index into a hybrid measure of ongoing biological activity, thereby diminishing its ability to identify individuals at risk *before* effector pathways become fully engaged.

This separation between susceptibility covariates (CMI, VAI, age, BMI, hypertension) and activation regulators (TyG, iPTH, AGR) is therefore not a methodological limitation but a conceptual necessity. It is important to distinguish between the predictable variables included in the FOSSI equations (selected for clinical practicality) and the exploratory biological drivers (TyG, iPTH), which provide mechanistic insight but are not part of the final prognostic indices. The strong associations observed between high FOSSI values and subsequent elevations in TyG, iPTH, or alterations in AGR provide internal validation of this framework, confirming that the susceptibility captured by FOSSI anticipates downstream biological activation and reinforcing the coherence and prognostic relevance of the index.

Notably, although the cardiometabolic index (CMI) contributed to risk stratification in both sexes, its role differed between men and women, as reflected by opposite regression signs in the female and male FOSSI equations. In men, a negative CMI coefficient suggests that accelerated ossification is less tightly linked to a classical insulin-resistant lipid profile and instead appears to coincide with a shift toward inflammatory and endocrine drivers. In women, by contrast, a positive association between CMI and FOSSI indicates that dyslipidaemia and central adiposity remain key metabolic contributors to susceptibility. This divergence highlights that, although the ossific outcome is shared, the underlying biological pathways leading to fast ossification differ meaningfully between men and women.

#### **4.4 Clinical implications**

Non-linear analysis reveals that FOSSI operates along two interpretable axes: as a predictor of clinical FO phenotype and as a normalised indicator of latent biological activation. In women, the gradual sigmoidal curve of FOSSI-F indicates a prolonged activation and

metabolic accumulation phase, resulting in a wider intervention window of approximately 8.3 years. It indicates an extended period during which metabolic factors remain dynamically associated with disease trajectory. In contrast, men show an abrupt activation pattern with a compressed window for modulation (approximately 3.4 years).

It could suggest that the involvement of inflammatory–endocrine pathways accelerates mineralisation more quickly than insulin resistance-driven pathways. However, another plausible explanation is the role of age. In men, age was found to be the dominant contributor in Shapley analyses of FOSSI-M, accounting for 56.8% of the total variance. Therefore, biological ageing itself acts as a powerful amplifier of susceptibility, potentially precipitating a rapid transition to accelerated ossification once a critical threshold is reached. This age-driven effect is consistent with the narrow intervention window identified in men, where relatively minor additional perturbations may be sufficient to trigger FO. In contrast, FOSSI-F in women appears to require the convergence of multiple upstream ossifying pressures, including metabolic dysregulation, visceral adiposity and cardiometabolic burden, before activation occurs. This cumulative process could influence the broader intervention window observed in women, indicating that FO activation reflects the integration of several concurrent susceptibility signals rather than the dominance of a single driver.

From a practical perspective, FOSSI-M may flag middle-aged men approaching accelerated variant in the context of subclinical inflammatory or vascular burden, while FOSSI-F may help identify postmenopausal women with high insulin resistance who could benefit from early metabolic assessment or lifestyle optimisation. Because FOSSI can be recalculated over time, changes in score trajectories may serve as early warning signals, supporting dynamic and individualised follow-up rather than static risk categorisation.

#### **4.5 FOSSI and Bone Quality**

Beyond its role in predicting accelerated ossification, FOSSI provides critical insight into the parallel deterioration of trabecular bone quality. The consistent inverse correlation between both FOSSI-F and FOSSI-M with the TBS –a direct index of bone microarchitecture– links high metabolic-osteogenic susceptibility to latent skeletal fragility. This relationship is biologically coherent: in women, FOSSI-F’s association with insulin resistance and visceral adiposity aligns with known mechanisms of glucose-driven oxidative stress and inflammation that impair osteoblast function and promote trabecular thinning [\[29\]](#). In men,

FOSSI-M's alignment with inflammatory-endocrine pathways (e.g., elevated iPTH and CTX) suggests a catabolic bone state characterized by increased resorption. Importantly, the suppression of bone formation markers (P1NP) in high FOSSI-F women further indicates a low-turnover phenotype, potentially compounding fracture risk in a manner distinct from traditional osteoporosis. Thus, FOSSI transcends a mere predictor of radiographic progression; it serves as a composite biomarker of a systemic "bone quality deficit" that accompanies the DISH phenotype.

#### **4.6 Methodological considerations**

Risk categories derived from FOSSI were intentionally framed using conservative, cohort-bound terminology. Accordingly, thresholds are described in terms of probability strata within this cohort rather than as diagnostic categories. Intermediate values are explicitly referred to as a "grey zone", indicating insufficient predictive certainty and that the primary intended use is for hypothesis generation and risk stratification in research settings.

It could be conjectured that constraining the model to PS-derived upstream covariates entailed any loss of discriminative performance when compared with a fully saturated, data-driven approach. In this context, we tested a comprehensive, unrestricted logistic model including all available metabolic and biochemical variables. Its AUC (0.84) did not exceed that of FOSSI-F and was nearly identical to FOSSI-M, reinforcing the advantages of a parsimonious, causally anchored approach.

FOSSI differs conceptually from conventional composite indices (CIs). Whereas CIs typically combine heterogeneous clinical events -often with limited causal coherence- FOSSI emerges from a recalibration of the propensity score using biologically anchored variables. This results in a substantially higher degree of biological consistency. CIs may aggregate outcomes that are not mechanistically related, but FOSSI assigns weights along plausible pathophysiological axes such as metabolic dysfunction and inflammation [30-32]. Moreover, its coefficients are derived from regression on a mechanistically constrained subset, paralleling the logic used in the development of FRAX [33].

Within current advances in PS methodology, FOSSI can be situated in the emerging field of causality-based predictive modelling, which views the propensity score as a conceptual bridge between causal inference and clinical prediction. Three elements of this framework are particularly relevant to FOSSI. First, a shared architecture with prognostic models: both condense multidimensional determinants into a single dimension of biological

vulnerability. Second, causal consistency: the same covariates used for confounder adjustment can be repurposed for clinically interpretable risk stratification without compromising the causal structure of the model. Third, biological plausibility: restricting predictors to covariates with established causal or mechanistic links reduces overfitting and enhances interpretability [15,30].

#### **4.7 Future Directions**

Our findings, together with prior evidence from the Camargo Cohort [6], suggest that the Fast Ossifier phenotype may represent more than an accelerated skeletal process. Two observations motivate this possibility: first, the co-occurrence of accelerated ossification and rapid trabecular deterioration in individuals with FO status; and second, the higher prevalence of heart failure, ischaemic heart disease, stroke, and use of anticoagulants, among subjects with elevated PS or FOSSI.

These associations raise an important mechanistic question: whether the biological susceptibility captured by FOSSI, rather than an isolated osteogenic process, reflects a parallel vulnerability across skeletal, metabolic, and vascular compartments.

In this context, FOSSI may extend beyond stratification of the ossification risk and serve as an indicator of broader systemic vulnerability within the DISH spectrum. Future longitudinal studies should therefore evaluate whether FOSSI identifies individuals at increased risk of metabolic or vascular deterioration, independently of its role in predicting skeletal progression. If supported by external validation, this framework could facilitate earlier recognition of patients prone to multi-system involvement and inform integrated preventive strategies addressing bone, metabolic, and vascular health.

#### **4.8 Limitations and strengths**

This study has limitations. The limited number of FO cases, particularly after sex stratification, represents an inherent constraint and warrants cautious interpretation. This limitation may increase the risk of overfitting and reduce the precision of coefficient estimates. However, FOSSI was intentionally conceived as a parsimonious risk-stratification tool, anchored to a small set of upstream variables, rather than as a high-dimensional predictive model. Accordingly, biological coherence and internal validation were prioritised over maximal model complexity. Within this framework, the convergence

of biologically plausible associations and statistically significant findings across complementary analytical approaches could support the internal consistency and robustness of the results.

The FO phenotype and the FOSSI indices require replication in larger and ethnically diverse populations, and reliance on a single cohort limits generalisability. Although causal inference cannot be fully established within an observational framework, the variables included in FOSSI originate directly from the longitudinal and mechanistic architecture that defines the FO framework. This provides the model with causal coherence and biological plausibility, distinguishing FOSSI from purely cross-sectional or data-driven prediction tools.

Nevertheless, the study has some positive aspects. These include its longitudinal design, sex-specific modelling strategy, and rigorous internal validation procedures, together with the convergence of clinical, biochemical, and imaging markers that support the internal consistency of the indices. By recalibrating the structure of the PS into a prognostic instrument, FOSSI remains aligned with the established causal drivers of accelerated ossification while providing an interpretable and transparent tool for early risk stratification. This integration of biologically anchored covariates with a reproducible statistical framework enhances the translational relevance of the work and provides a solid foundation for future external validation.

## **5. CONCLUSIONS**

FOSSI-F and FOSSI-M demonstrated excellent discrimination and robust internal validity. Their sex-specific cut-offs identified individuals at elevated risk of transitioning to FO status, years before skeletal, vascular, or metabolic complications become clinically detectable. In addition, the intervention-window estimates (3.4 years in men; 8.3 years in women) offer a practical margin for targeted prevention.

By selectively capturing the latent signal embedded within the propensity score, both indices uncovered clear sex-specific pathways: an insulin-resistance/visceral-adiposity axis in women and inflammatory–endocrine drivers in men.

FOSSI bridges domains rarely integrated in bone research. Simultaneously anchored to the FO phenotype and to the underlying PS structure, it connects bone quality, axial ossification, turnover dynamics, iPTH, glucose–lipid alterations, anthropometrics, insulin

resistance, and systemic inflammation, providing a coherent framework for the metabolic–vascular–osteogenic continuum characteristic of DISH.

Methodologically, this work delivers two advances: one of the first sex-specific prognostic instruments for DISH, and a demonstration that PS-derived modelling can be translated into a clinically interpretable index aligned with personalised medicine.

While external validation is required prior to clinical implementation, FOSSI-F and FOSSI-M provide a validated, parsimonious framework for risk stratification in research settings and highlight critical sex-specific pathways for mechanistic investigation.

## REFERENCES

- [1] Pini SF, Pariente E, Olmos JM, Martín-Millán M, Pascua R, Martínez-Taboada VM, Hernández JL. Diffuse idiopathic skeletal hyperostosis (DISH) and trabecular bone score (TBS) in postmenopausal women: The Camargo cohort. *Semin Arthritis Rheum*. 2023 Aug;61:152217. doi: 10.1016/j.semarthrit.2023.152217.
- [2] Mader R, Novofastovski I, Schwartz N, Rosner E. Serum adiponectin levels in patients with diffuse idiopathic skeletal hyperostosis (DISH). *Clin Rheumatol*. 2018 Oct;37(10):2839-2845. doi: 10.1007/s10067-018-4258-0.
- [3] Harlianto NI, Oosterhof N, Foppen W, Hol ME, Wittenberg R, van der Veen PH, et al.; UCC-SMART-Studygroup. Diffuse idiopathic skeletal hyperostosis is associated with incident stroke in patients with increased cardiovascular risk. *Rheumatology (Oxford)*. 2022 Jul 6;61(7):2867-2874. doi: 10.1093/rheumatology/keab835.
- [4] Murakami Y, Morino T, Hino M, Misaki H, Miura H. Progression of Ossification of the Anterior Longitudinal Ligament Associated With Diffuse Idiopathic Skeletal Hyperostosis by Age: A Study of Computed Tomography Findings Over 5 Years. *Global Spine J*. 2021 Jun;11(5):656-661. doi: 10.1177/2192568220918817.
- [5] Brikman S, Lubani Y, Mader R, Bieber A. High prevalence of diffuse idiopathic skeletal hyperostosis (DISH) among obese young patients - A retrospective observational study. *Semin Arthritis Rheum*. 2024 Apr;65:152356. doi: 10.1016/j.semarthrit.2023.152356.
- [6] Pariente-Rodrigo E, Martín-Millán M, Sgaramella G, Pardo-Lledías J, Fierro-Andrés P, Bonome M, et al. 'Fast Ossifier' in diffuse idiopathic skeletal hyperostosis: a sex-modulated, heterogeneous phenotype with accelerated ossification and early trabecular decline. *RMD Open*. 2025 Sep 21;11(3):e006024. doi: 10.1136/rmdopen-2025-006024.
- [7] Aletaha D, Smolen JS. Diagnosis and Management of Rheumatoid Arthritis: A Review. *JAMA*. 2018 Oct 2;320(13):1360-1372. doi: 10.1001/jama.2018.13103. PMID: 30285183.
- [8] Smolen JS, Landewé RBM, Bergstra SA, Kerschbaumer A, Sepriano A, Aletaha D, et al. EULAR recommendations for the management of rheumatoid arthritis with synthetic and biological disease-modifying antirheumatic drugs: 2022 update. *Ann Rheum Dis*. 2023 Jan;82(1):3-18. doi: 10.1136/ard-2022-223356.
- [9] Janke K, Kiefer C, McGauran N, Richter B, Krause D, Wieseler B. A systematic comparison of different composite measures (DAS 28, CDAI, SDAI, and Boolean approach) for determining

treatment effects on low disease activity and remission in rheumatoid arthritis. *BMC Rheumatol.* 2022 Dec 9;6(1):82. doi: 10.1186/s41927-022-00314-7.

[10] Ramiro S, Nikiphorou E, Sepriano A, Ortolan A, Webers C, Baraliakos X, et al. ASAS-EULAR recommendations for the management of axial spondyloarthritis: 2022 update. *Ann Rheum Dis.* 2023 Jan;82(1):19-34. doi: 10.1136/ard-2022-223296.

[11] Coates LC, Soriano ER, Corp N, Bertheussen H, Callis Duffin K, et al. GRAPPA Treatment Recommendations domain subcommittees. Group for Research and Assessment of Psoriasis and Psoriatic Arthritis (GRAPPA): updated treatment recommendations for psoriatic arthritis 2021. *Nat Rev Rheumatol.* 2022 Aug;18(8):465-479. doi: 10.1038/s41584-022-00798-0.

[12] Glynn RJ, Schneeweiss S, Stürmer T. Indications for propensity scores and review of their use in pharmacoepidemiology. *Basic Clin Pharmacol Toxicol.* 2006;98(3):253–259. doi:10.1111/j.1742-7843.2006.pto\_329.x.

[13] Leacy FP, Stuart EA. On the joint use of propensity and prognostic scores in estimation of the average treatment effect on the treated: a simulation study. *Stat Med.* 2014;33(20):3488-508. doi:10.1002/sim.6030.

[14] Yang JY, Webster-Clark M, Lund JL, Sandler RS, Dellon ES, Stürmer T. Propensity score methods to control for confounding in observational cohort studies: a statistical primer and application to endoscopy research. *Gastrointest Endosc.* 2019;90(3):360-369. doi:10.1016/j.gie.2019.04.236.

[15] Jackson JW, Schmid I, Stuart EA. Propensity Scores in Pharmacoepidemiology: Beyond the Horizon. *Curr Epidemiol Rep.* 2017 Dec;4(4):271-280. doi: 10.1007/s40471-017-0131-y.

[16] Hernández JL, Olmos JM, Pariente E, Martínez J, Valero C, García-Velasco P, et al. Metabolic syndrome and bone metabolism: the Camargo Cohort study. *Menopause.* 2010 Sep-Oct;17(5):955-61. doi: 10.1097/gme.0b013e3181e39a15.

[17] Schlapbach P, Beyeler C, Gerber NJ, van der Linden S, Bürgi U, Fuchs WA, et al. Diffuse idiopathic skeletal hyperostosis (DISH) of the spine: a cause of back pain? A controlled study. *Br J Rheumatol.* 1989 Aug;28(4):299-303. doi: 10.1093/rheumatology/28.4.299.

[18] Pini SF, Acosta-Ramón V, Tobalina-Segura M, Pariente-Rodrigo E, Rueda-Gotor J, Olmos-Martínez JM, et al. Interobserver agreement using Schlapbach graded scale for diffuse idiopathic skeletal hyperostosis (DISH): can we reduce the cut-off point of vertebral affection? *Clin Rheumatol.* 2019 Apr;38(4):1155-1162. doi: 10.1007/s10067-018-4398-2.

[19] Steyerberg, Ewout W. "Validation of prediction models." *Clinical prediction models: a practical approach to development, validation, and updating.* Cham: Springer International Publishing, 2019. 329-344.

[20] Bi J. A review of statistical methods for determination of relative importance of correlated predictors and identification of drivers of consumer liking. *J Sensory Studies.* 2012;27(2):87-101. doi:10.1111/j.1745-459X.2012.00370.x.

[21] Montesinos-López OA, Montesinos-López A, Pérez-Rodríguez P, de los Campos G, Eskridge KM, Crossa J. *Multivariate Statistical Machine Learning Methods for Genomic Prediction.* Cham (CH): Springer; 2022. Chapter 4: Overfitting, Model Tuning, and Evaluation of Prediction Performance. doi:10.1007/978-3-030-89010-0\_4.

[22] Ciarambino T, Crispino P, Guarisco G, Giordano M. Gender Differences in Insulin Resistance: New Knowledge and Perspectives. *Curr Issues Mol Biol.* 2023;45(10):7845-7861. doi:10.3390/cimb45100496.

- [23] Conte C, Epstein S, Napoli N. Insulin resistance and bone: a biological partnership. *Acta Diabetol.* 2018 Apr;55(4):305-314. doi: 10.1007/s00592-018-1101-7.
- [24] Ho CY, Shanahan CM. Medial Arterial Calcification: An Overlooked Player in Peripheral Arterial Disease. *Arterioscler Thromb Vasc Biol.* 2016 Aug;36(8):1475-82. doi: 10.1161/ATVBAHA.116.306717.
- [25] Epsley S, Tadros S, Farid A, Kargilis D, Mehta S, Rajapakse CS. The Effect of Inflammation on Bone. *Front Physiol.* 2021;11:511799. doi:10.3389/fphys.2020.511799.
- [26] Shieh A, Greendale GA, Cauley JA, Srikanthan P, Karlamangla AS. Longitudinal associations of insulin resistance with change in bone mineral density in midlife women. *JCI Insight.* 2022 Oct 24;7(20):e162085. doi:10.1172/jci.insight.162085.
- [27] McLaughlin T, Abbasi F, Cheal K, Chu J, Lamendola C, Reaven G. Use of metabolic markers to identify overweight individuals who are insulin resistant. *Ann Intern Med.* 2003 Nov 18;139(10):802-9. doi: 10.7326/0003-4819-139-10-200311180-00007.
- [28] Sun Y, Ji H, Sun W, An X, Lian F. Triglyceride glucose (TyG) index: A promising biomarker for diagnosis and treatment of different diseases. *Eur J Intern Med.* 2025 Jan;131:3-14. doi: 10.1016/j.ejim.2024.08.026.
- [29] Lin Y, Zhong X, Lu D, Yao W, Zhou J, Wu R, et al. Association of visceral and subcutaneous fat with bone mineral density in US adults: a cross-sectional study. *Sci Rep.* 2023 Jul 1;13(1):10682. doi: 10.1038/s41598-023-37892-6.
- [30] Hansen, B. The prognostic analogue of the propensity score. *Biometrika.* 2008;95(2), 481-488. doi:10.1093/biomet/asn004.
- [31] McKenna SP, Heaney A. Composite outcome measurement in clinical research: the triumph of illusion over reality? *J Med Econ.* 2020;23(10):1196-1204. doi:10.1080/13696998.2020.1797755.
- [32] McCoy CE. Understanding the Use of Composite Endpoints in Clinical Trials. *West J Emerg Med.* 2018;19(4):631-634. doi:10.5811/westjem.2018.4.38383.
- [33] Kanis JA, Johnell O, Oden A, Johansson H, McCloskey E. FRAX™ and the assessment of fracture probability in men and women from the UK. *Osteoporos Int.* 2008;19(4):385-397. doi:10.1007/s00198-007-0543-5.



**Table 1:** Characteristics of FOSSI-F (females) and FOSSI-M (males)

FOSSI-F		FO phenotype: Probability stratum (within cohort)	R <sup>2</sup> contribution (Shapley method)	Equation
Score range	< 5.84	Low	Age (41.6 %), BMI (32.2 %), CMI (14.4 %), VAI (10.5 %), Hypertension (1.3 %)	-18.811 + (0.209 × age) + (0.350 × BMI) + (1.359 × CMI) + (0.203 × VAI) + (0.799 × hypertension)
	5.84 – 7.88	Intermediate		
	7.89 – 9.58	High		
	> 9.58	Very high		

FOSSI-M		FO phenotype: Probability stratum (within cohort)	R <sup>2</sup> contribution (Shapley method)	Equation
Score range	< 0.71	Low	Age (56.8 %), WC (17.9 %), CMI (12.8 %), BMI (12.5 %)	-4.663 + (0.039 × age) + (0.015 × WC) - (0.223 × CMI) + (0.045 × BMI)
	≥ 0.71	High		

The reduced number of probability strata in FOSSI-M reflects the near-threshold distribution observed in men. Thresholds define internal probability strata within this cohort rather than diagnostic categories. Intermediate values represent a transitional ‘grey zone’, reflecting gradual biological activation. At this stage, these categories are intended for risk stratification and research-oriented interpretation. The table also shows the weighted influence of each included variable, normalised to sum to 100% using R<sup>2</sup> decomposition (Shapley analysis).

FO: Fast Ossifier

BMI: Body mass index; WC: Waist circumference;

Hypertension: coded as 1=yes, 0=no;

CMI: Cardiometabolic index:  $[TG \text{ (mmol/L)} / HDL \text{ (mmol/L)}] \times [Waist \text{ circumference (cm)} / Height \text{ (cm)}]$

VAI: Visceral adiposity index (females):  $[WC \text{ (cm)} / (36.58 + (1.89 \times BMI))] \times [TG \text{ (mmol/L)} / 0.81] \times [1.52 / HDL \text{ (mmol/L)}]$

**Table 2:** Diagnostic performance and internal validity of the FOSSI-F and FOSSI-M equations for the identification of the Fast Ossifier (FO) phenotype

EQUATION	STRATUM	OR (95% CI)	<i>p</i> -value	AUC (95% CI)	Youden J	SE (%)	SP (%)	PPV (%)	NPV (%)	Spearman correlation
<b>FOSSI-F</b>	Females	10.2 (3.3-31)	< 0.001	0.875 (0.77-0.97)	0.616	83.3	78.3	70	88.5	0.685
	Females < 66 years	17.3 (3.3-89)	< 0.001	0.913 (0.69-0.95)	0.690	87.5	81.5	63.6	95.1	0.732
	Females ≥ 66 years	6.95 (1.5-32)	< 0.001	0.820 (0.65-0.89)	0.528	77.8	75	63.8	85.7	0.621
<b>FOSSI-M</b>	Males	5.58 (2.6-11)	< 0.001	0.836 (0.75-0.91)	0.550	81.8	73.2	61.4	88.5	0.611
	Males < 66 years	6.97 (2.2-2.9)	< 0.001	0.857 (0.76-0.95)	0.590	84.6	74.4	61.1	91.1	0.644
	Males ≥ 66 years	4.58 (1.6-13)	0.004	0.813 (0.68-0.93)	0.497	78.6	71.1	61.1	85.7	0.582

*Odds ratios (OR) with 95% confidence intervals and p-values are reported for the association with FO. Discriminative ability was evaluated using the area under the ROC curve (AUC, 95% CI). The Youden index and derived parameters (sensitivity [SE], specificity [SP], positive predictive value [PPV], and negative predictive value [NPV]) were calculated at empirically determined optimal thresholds. Convergent validity was assessed through the Spearman correlation coefficient.*

**Table 3**

Significant correlations between both FOSSI indices and metabolic biomarkers in different strata

	FOSSI - F			FOSSI - M		
	Females (N=483)	Females < 66 years (N=240)	Females ≥ 66 years (N=243)	Males (N=396)	Males < 66 years (N=184)	Males ≥ 66 years (N=212)
Propensity score	0.847**	0.821**	0.778**	0.859**	0.731**	0.798**
BMI	0.635**	0.804**	0.816**	0.484**	0.663**	0.665**
WC	0.549**	0.623**	0.598**	0.558**	0.673**	0.720**
TyG index	0.337**	0.463**	0.373**			
CMI	0.471**	0.660**	0.566**			
VAI_F / VAI_M	0.333**	0.490**	0.403**			
AGR	- 0.107*			- 0.159**		- 0.138*
ALP				0.130**		
ALB	- 0.165**	- 0.133*		- 0.155**		- 0.150*
iPTH	0.236**		0.214**	0.176**		0.140*
P1NP	- 0.145**	- 0.260**				
CTX	- 0.178**	- 0.292**			0.183*	
TBS	- 0.499**	-0.502**	- 0.504**	- 0.359**	- 0.400**	- 0.447**

\* $p < 0.05$ ; \*\* $p < 0.01$ . Only correlations reaching statistical significance are shown.

P1NP: aminoterminal propeptide of type 1 collagen; CTX: C-terminal telopeptide of type 1 collagen; iPTH: intact parathormone; TBS: trabecular bone score; AGR: Albumin-to-globulin ratio; TyG: Triglyceride-glucose index; ALP: alkaline phosphatase; ALB: albumin; BMI: Body mass index; WC: waist circumference; CMI: cardiometabolic index; VAI: Visceral adiposity index (F: female; M: male).

FOSSI-F and FOSSI-M show significant correlations with key metabolic and skeletal parameters. FOSSI-F is more strongly associated with insulin resistance (TyG, CMI), visceral adiposity, and suppressed bone turnover (P1NP, CTX), whereas FOSSI-M correlates with inflammatory profiles and increased bone resorption (CTX). Both indices show an inverse correlation with trabecular bone score (TBS), linking them to subclinical skeletal degradation.

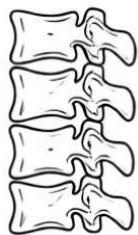
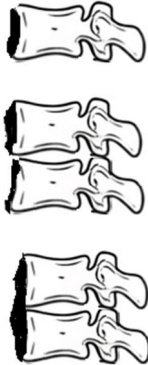


**Table 4:** Prevalence of covariates according to FOSSI-F and FOSSI-M distribution strata defined by tertiles

	FOSSI - F				FOSSI - M			
	Lowest tertile	Medium tertile	Highest tertile	p-value	Lowest tertile	Medium tertile	Highest tertile	p-value
Metabolic syndrome; n(%)	50 (19.7)	83 (32.7)	121 (47.6)	0.0001	59 (26.9)	73 (33.3)	87 (39.7)	0.001
T2DM; n(%)	18 (24)	22 (29.3)	35 (46.7)	0.009	24 (23.3)	37 (35.9)	42 (40.8)	0.012
Hypertension; n(%)	73 (25.7)	103 (36.3)	109 (38.8)	0.0001	68 (28)	85 (35)	40 (37)	0.005
Obesity; n(%)	44 (16.9)	79 (30.3)	138 (52.9)	0.0001	32 (18.7)	56 (32.7)	83 (48.5)	0.0001
Heart failure; n(%)	2 (20)	5 (50)	3 (30)	0.15	2 (10)	6 (30)	12 (60)	0.0004
Ischemic heart disease; n(%)	2 (12.5)	5 (31.3)	9 (56.3)	0.029	13 (24.5)	16 (30.2)	24 (45.3)	0.047
Stroke; n(%)	2 (22.2)	3 (33.3)	4 (44.4)	0.41	5 (21.7)	6 (26.1)	12 (52.2)	0.06
WC >108 cm**; n(%)	17 (12.3)	43 (31.2)	78 (56.5)	0.0001	14 (10.9)	39 (30.2)	76 (58.9)	0.0001
TyG index >8.79**; n(%)	28 (20)	45 (32.1)	67 (47.9)	0.0001	57 (38.8)	49 (33.3)	41 (27.9)	0.08
ALP >78 U/L**; n(%)	57 (30.5)	59 (31.6)	71 (38)	0.21	31 (29.8)	31 (29.8)	42 (40.4)	0.046
iPTH >62 pg/mL**; n(%)	34 (21.7)	52 (33.1)	71 (45.2)	0.0001	27 (22.3)	41 (33.9)	53 (43.8)	0.003
CMI >0.73**; n(%)	12 (10.4)	34 (29.6)	69 (60)	0.001	52 (39.7)	42 (32.1)	37 (28.2)	0.52
VAI >2.10**; n(%)	25 (16.4)	49 (31.2)	78 (51.3)	0.0001	50 (39.4)	44 (34.6)	33 (26)	0.21
AGR <1.50*; n(%)	45 (28.5)	55 (34.8)	58 (36.7)	0.06	32 (25.4)	42 (33.9)	50 (40.3)	0.029
P1NP <31.23 ng/mL* n(%)	28 (17.4)	49 (30.4)	46 (28.6)	0.008	59 (44.7)	63 (47.7)	47 (35.6)	0.14
CTX <0.22 ng/mL* n(%)	27 (17)	46 (29.9)	49 (31.4)	0.001	45 (35.7)	47 (37.6)	49 (39.1)	0.46
Trabecular bone score <1.230; n(%)	11 (8.7)	35 (27.6)	81 (63.8)	0.0001	22 (22)	26 (26)	52 (52)	0.0001
Thiazides; n(%)	44 (23.7)	66 (35.5)	76 (40.9)	0.0001	16 (19.3)	24 (28.9)	43 (51.8)	0.0001
Anticoagulants; n(%)	7 (12.3)	21 (36.8)	29 (50.9)	0.0001	3 (15)	4 (20)	13 (65)	0.0001
Insulin; n(%)	4 (19)	5 (23.8)	12 (57.1)	0.029	5 (35.7)	6 (42.9)	3 (21.4)	0.50
Antidiabetics; n(%)	14 (22.2)	18 (28.6)	31 (49.2)	0.005	19 (25)	27 (35.5)	30 (39.5)	0.08
Statins; n(%)	24 (18.3)	56 (42.7)	51 (38.9)	0.001	48 (31.8)	51 (33.8)	52 (34.4)	0.61

\*Cut-off point for lowest tertile;\*\*Cut-off point for highest tertile; WC: Waist circumference; TyG: Triglycerides Glucose index; ALP: Alkaline phosphatase; iPTH: Intact Parathormone; CMI: Cardiometabolic index; VAI: Visceral adiposity index; AGR: Albumin-to-globulin ratio.

This table highlights the clinical phenotypes associated with high FOSSI-F and FOSSI-M scores. In their upper tertiles, both indices concentrate FO cases and individuals with metabolic syndrome, central adiposity, elevated iPTH, and, in men, low albumin-to-globulin ratio (inflammation). These patterns reinforce the role of FOSSI as a multidimensional biomarker reflecting both endocrine-metabolic disruption and emerging skeletal risk.

**Figure 1:** Schlapbach's graded scale applied to DISH radiographs

<b>Grade 0:</b> No visible ossification, non-DISH	<b>Grade 1:</b> Prevertebral and/or prediscal ossification at one or two vertebral levels, or a single bridging ossification	<b>Grade 2:</b> Continuous prediscal and/or prevertebral ossification involving three or more vertebral levels, or two bridging ossifications	<b>Grade 3:</b> Three or more bony bridges
			

*The Schlapbach semi-quantitative graded scale demonstrates high methodological suitability for the assessment of axial ossification in DISH, combining strong reproducibility with robust construct validity. Previous studies have consistently reported good-to-excellent intra- and interobserver agreement, supporting its reliability for both cross-sectional classification and longitudinal follow-up. In a dedicated reliability analysis from our cohort, the scale showed good inter- and intraobserver agreement ( $\kappa \geq 0.81$  and  $\geq 0.85$ , respectively) confirming its robustness in routine clinical radiographs and supporting its applicability to early disease stages.*

**Figure 2:** Non-linear relationships between FOSSI and FO phenotype

**Figure 2A**

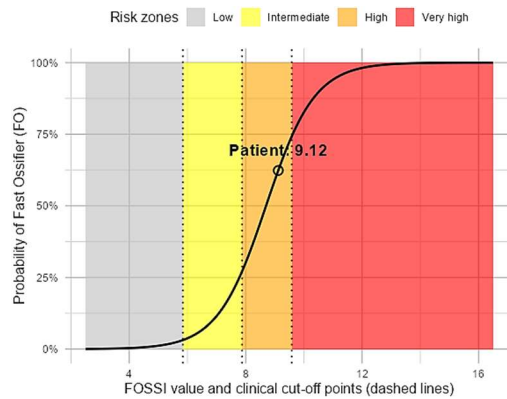


**Figure 2B**

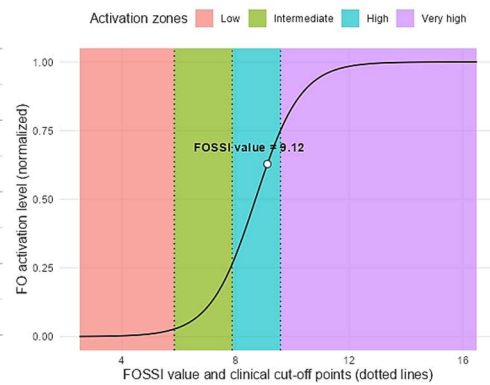


**Figure 2C**

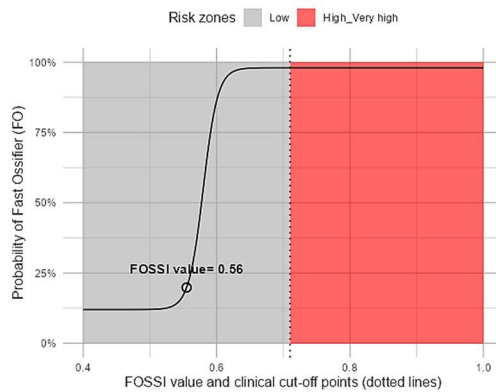
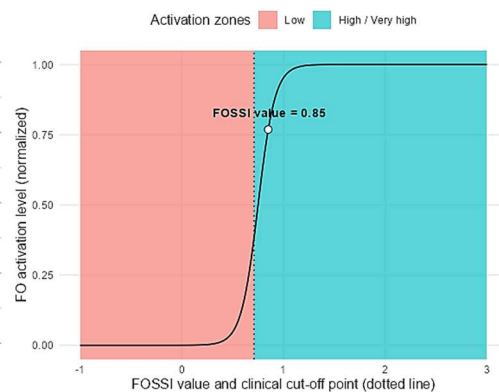


**Figure 2D**



**Figures 2A-2B.** Complementary projections of FOSSI-F in women. **(A)** Model-based probability of FO across the same FOSSI-F range. Shaded regions indicate clinically interpretable strata; the highlighted point illustrates the individual position under both projections. **(B)** Normalized activation curve depicting the degree of downstream osteoformative activation across the FOSSI-F continuum.

**2A:** FOSSI-F value projected onto FO status corresponds to a probability of FO near 75%.

**2B:** This value of 9.12 corresponds to Y value  $\approx 0.65-0.70$ , which indicates that a substantial part of the downstream bone-forming activation process is already completed.

Consequently, a FOSSI-F value of 9.12 places the individual within a high model-based probability of FO, as well as an advanced activation phase of the FO transformation process.

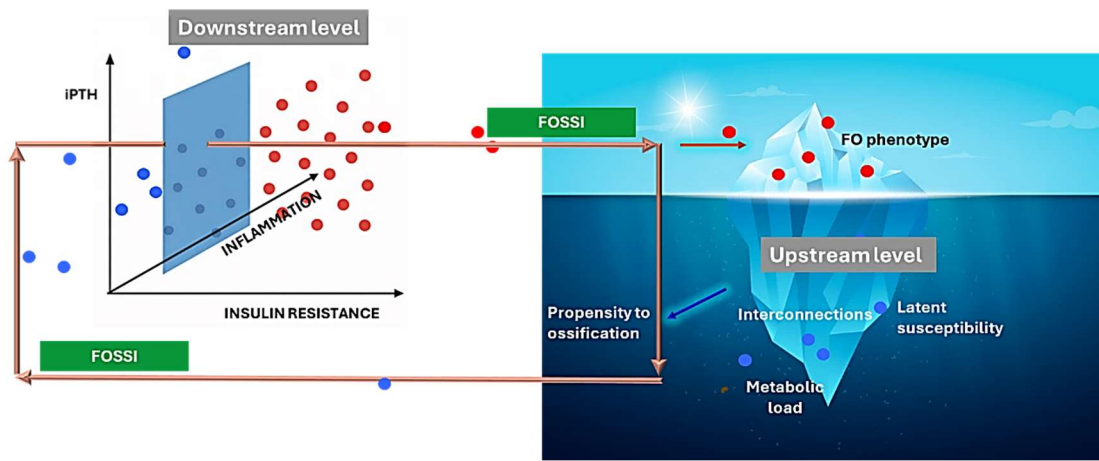
**Figures 2C-2D.** Complementary projections of FOSSI-M in men. **(C)** Corresponding model-based FO probability, demonstrating near-binary discrimination beyond the activation threshold. **(D)** Normalized activation curve showing an abrupt transition toward FO activation over a narrow FOSSI-M interval.

A FOSSI-M value of 0.56 places the individual at the onset of the process of transformation (near 20-25%) and when projected onto FO status, this position corresponds to a low probability of FO.

Together, the four panels demonstrate that FOSSI captures a continuous biological activation process whose statistical projection onto FO status yields sex-specific probability profiles.

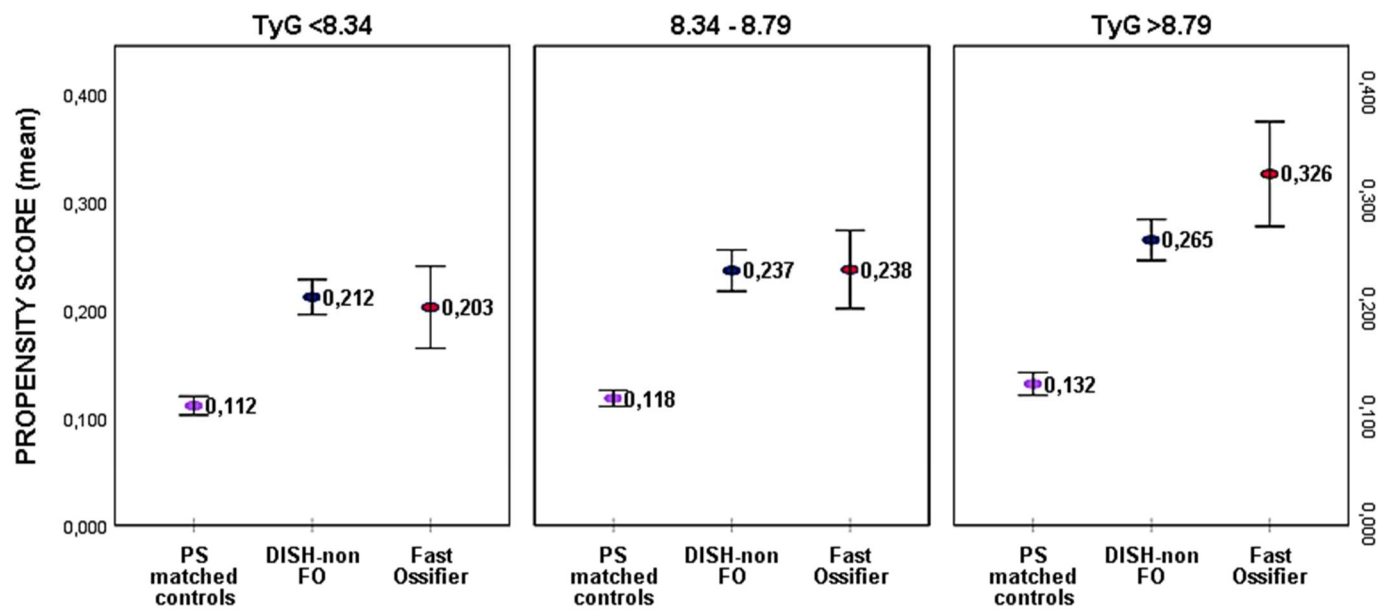
**Figure 3:**

Proposed dual-layer biological model linking FOSSI to the Fast Ossifier phenotype



*Schematic representation of the functional positioning of FOSSI within the DISH biological continuum. The diagram illustrates how FOSSI bridges latent susceptibility and phenotypic expression, integrating information from the metabolic background space and translating it into a measurable propensity to ossify. The spatial arrangement highlights the transition from subclinical biological tension to overt Fast Ossifier (FO) phenotype, emphasising the role of FOSSI as an intermediate transducer rather than a terminal outcome marker.*

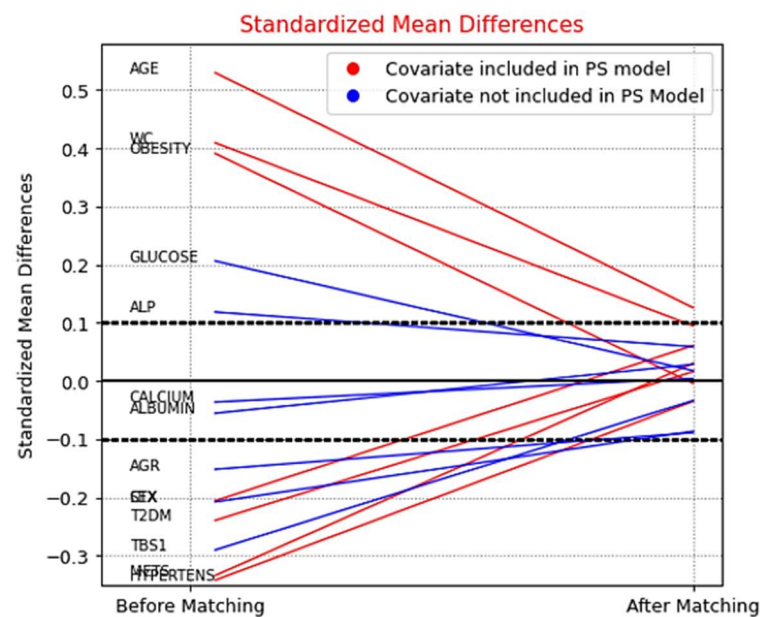
**Suppl. Mat., annex 1:** Propensity score, Fast Ossifier (FO) status and insulin resistance (TyG index tertiles)



TyG: Triglyceride Glucose index; FO: Fast Ossifier  
Elaborated with data from baseline, the figure illustrates the emerging clinical value of the propensity score (PS) beyond its traditional statistical role. Higher PS values are associated with both insulin resistance (IR, assessed via TyG index) and Fast Ossifier (FO) status, even in patients without radiographic ossification. Clinically, this suggests that the PS may capture a latent metabolic vulnerability preceding skeletal changes, supporting its reinterpretation as an early risk biomarker for accelerated ossification.



Suppl Mat, annex 2: Standardised mean differences before and after Propensity score matching



PSM Balance Assessment Report

Covariate	SMD Before	SMD After	VR Before	VR After
AGE	0.5292	0.1258	1.0063	0.8732
WC	0.4090	0.0945	0.8344	1.0466
OBESITY	0.3904	-0.0043	1.1285	1.0004
SEX	-0.2056	0.0606	1.0768	0.9948
T2DM	-0.2394	0.0160	1.5235	0.9770
METS	-0.3342	0.0304	1.0773	1.0044
HYPERTENS	-0.3422	-0.0349	1.0145	0.9906

	Before Matching	After Matching
Pseudo-R <sup>2</sup>	0.0573	-0.3230
L1 Imbalance	0.3500	0.0524

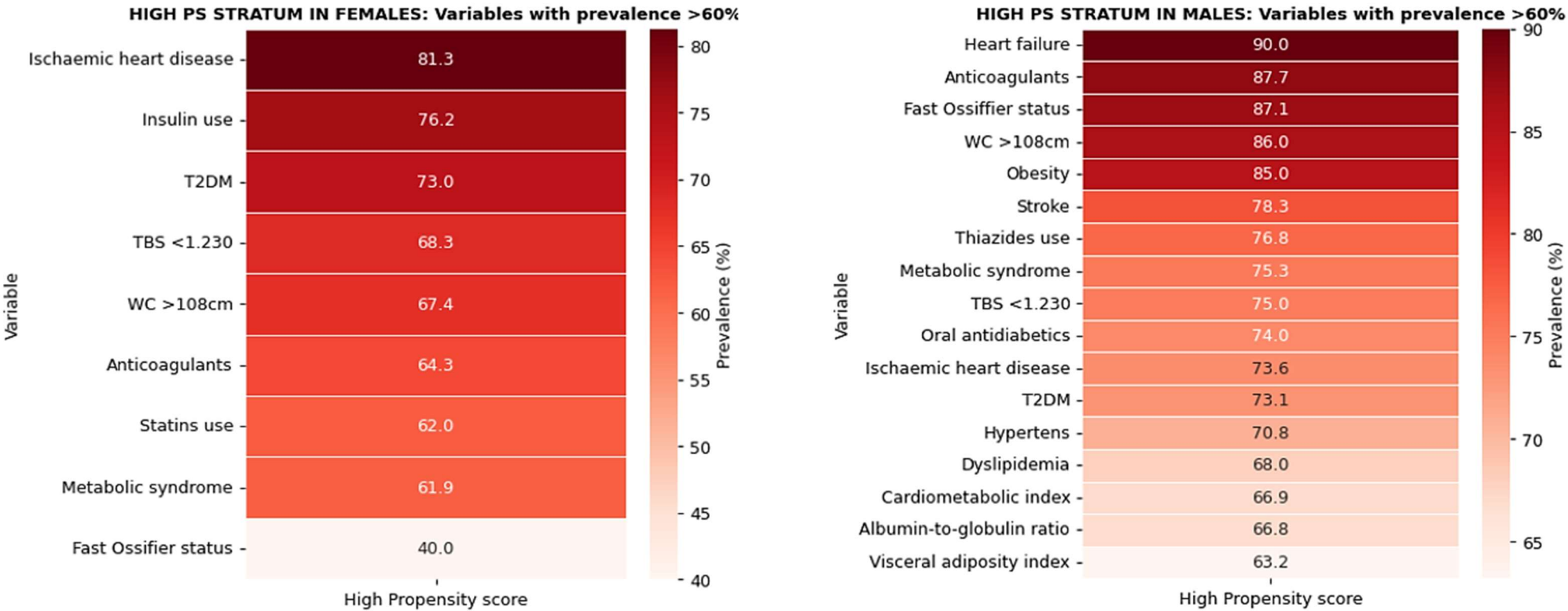
T2DM: Type 2 diabetes mellitus; WC: Waist circumference; MetS: Metabolic syndrome. SMD: Standardized Mean Difference. VR: Variance Ratio

Covariates included in PS model (red): Age, WC, obesity, sex, T2DM, MetS and hypertension.

Covariates not included in PS model (blue): Glucose, alkaline phosphatase (ALP), calcium, albumin, albumin-to-globulin ratio (AGR), CTX, and trabecular bone score (TBS1).

In addition to covariates included in the PS model, several metabolic, inflammatory, and skeletal variables not explicitly modelled also converged below conventional balance thresholds ( $|SMD| < 0.1$ ), suggesting that the PS captures a broader latent biological configuration beyond the selected covariates.

**Suppl. Mat., annex 3:** Propensity score- high stratum and variables showing elevated prevalence



Inspection of the high-propensity stratum revealed marked sex differences in PS architecture: whereas in men the PS captured a tightly clustered cardiometabolic–vascular–osteogenic environment in which FO was nearly ubiquitous, in women the PS identified a permissive metabolic vulnerability state, from which only a subset progressed to overt FO. Variables are shown for descriptive purposes only, illustrating sex-dependent clustering patterns encoded within the PS framework.

#### Suppl. Mat., annex 4: Assessment of Comparability between Fast Ossifiers and Non-Progressors

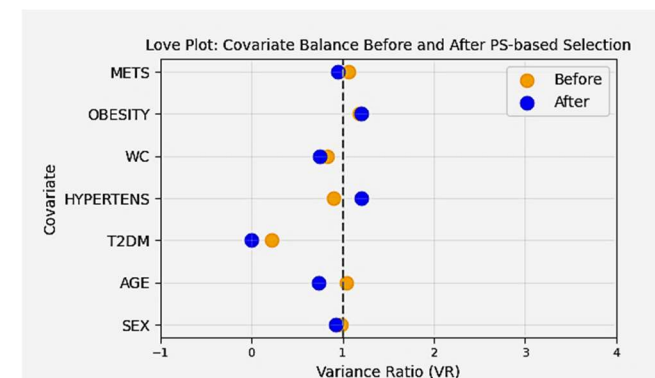
Both groups, originated from the same PS-enriched subcohort of non-DISH individuals, provide high baseline homogeneity in metabolic covariates and ensure a shared risk structure. Baseline comparability between Fast Ossifiers (FO) and non-progressors (NP) was assessed using three complementary balance diagnostics: standardized mean differences (SMD), variance ratios (VR), and McFadden's pseudo- $R^2$ .

**SMD values** demonstrated excellent balance for MetS ( $|SMD| < 0.1$ ) and acceptable ( $\leq 0.30$ ) for obesity, hypertension, WC, with residual imbalance addressed by analytical adjustment. These demographic covariates were therefore adjusted analytically in all prognostic models, consistent with best practices in prognostic modelling. **Variance ratios**, which evaluate dispersion overlap, fell within Rubin's accepted range (0.5–2.0) for all covariates, with the majority (Sex, obesity, hypertension, METS) also within the stricter 0.8–1.25 criterion. WC and age showed acceptable dispersion overlap. T2DM exhibited a  $VR \approx 0$ , reflecting near-zero variability within one group, consistent with its limited prognostic relevance. **McFadden's pseudo- $R^2$**  decreased markedly after PS-based subcohort selection (from 0.1068 to 0.0457), indicating reduced baseline separability and supporting adequate covariate overlap.

According to the assessment, this group composed of FO and NP and derived from the initial matching, preserved the original high balance obtained by using the PS, and was methodologically adequate for prognostic model development.

The table shows the SMD and VR-specific values before and after the group was formed. The love plot illustrates the improved dispersion balance after PS-based selection.

Covariate	SMD Before	SMD After	VR Before	VR After
SEX	-0.054	-0.216	0.984	0.923
AGE	0.538	0.375	1.036	0.740
T2DM	0.344	0.381	0.220	0.000
HYPERTENS	-0.567	0.295	0.898	1.200
WC	0.390	0.424	0.829	0.744
OBESITY	0.475	0.295	1.184	1.200
METS	-0.059	0.075	1.059	0.950



T2DM: Type 2 diabetes mellitus; WC: Waist circumference; MetS: Metabolic syndrome. SMD: Standardized Mean Difference. VR: Variance Ratio

It should be noted that the balance diagnostics reported in this annex assess comparability between Fast Ossifiers and Non-Progressors within the PS-enriched analytical cohort, and therefore differ conceptually from the SMD shown in Supplementary Annex 2, which illustrate the effect of PS-based selection on the overall covariate space before and after matching.

**Suppl. Mat., annex 5: Multivariable modelling of FOSSI-F and FOSSI-M**

EQUATION	Modelling	Independent variable	Dependent variable	Result	p	Adjustment	Model fit / Effect size
FOSSI-F	ANCOVA		FOSSI-F	Estimated FOSSI-F means (95% CI): * FO cases = 7.62 (6.8 - 8.4) * Controls = 5.54 (5.1 - 5.8)	0.0001	Charlson index, TyG, MetS, CMI, BMI, WC, HDL, iPTH, TBS, Alkaline phosphatase, Albumin, Hypertension, T2DM, Obesity, Statins or antidiabetics use	R <sup>2</sup> = 0.785 Eta-squared = 0.224
	Multivariable logistic regression	FOSSI-F	FO status	[FOSSI-F] Adjusted OR = 2.50 (95%CI: 1.4 - 4.2)	0.001	Obesity, DLP, T2DM, Hypertension, Statins or antidiabetics use, Albumin, iPTH, P1NP, CTX, 25(OH)D	R <sup>2</sup> = 0.603
	Shapley R <sup>2</sup> decomposition	FOSSI-F	LMG values (normalized to sum 100%): <ul style="list-style-type: none"> <li>TyG index = 0.798 (79.8 %)</li> <li>iPTH = 0.193 (19.3%)</li> <li>AGR = 0.008 (0.8 %)</li> </ul>				
FOSSI-M	ANCOVA		FOSSI-M	Estimated FOSSI-M means (95%CI): * FO cases = 0.78 (0.6 - 0.8) * Controls = 0.23 (0.2 - 0.3)	0.0001	Charlson index, TyG, MetS, CMI, BMI, WC, HDL, iPTH, TBS, Alkaline phosphatase, Statins or antidiabetics use, AGR, Ca × P	R <sup>2</sup> = 0.214 Eta-squared = 0.557
	Univariate logistic regression	FOSSI-M	FO status	[FOSSI-M] OR = 1.36 (95%CI: 1.02 - 1.8)	0.035		
	Shapley R <sup>2</sup> decomposition	FOSSI-M	LMG values (normalized to sum 100%): <ul style="list-style-type: none"> <li>iPTH = 0.595 (59.5 %)</li> <li>TyG index = 0.245 (24.5 %)</li> <li>AGR = 0.161 (16.1 %)</li> </ul>				

Results of regression models are presented, indicating the independent and dependent variables, estimated coefficients, and levels of statistical significance (p). Adjusted models included relevant clinical and metabolic covariates. Overall model fit and effect size are expressed using goodness-of-fit statistics or explained variance measures, as appropriate.

MetS: Metabolic syndrome; T2DM: Type 2-diabetes mellitus; BMI: Body mass index; CMI: Cardiometabolic index; P1NP: aminoterminal propeptide of type 1 collagen; CTX: C-terminal telopeptide of type 1 collagen; iPTH: intact parathormone; WC: Waist circumference; HDL: High-density lipoproteins cholesterol; TBS: trabecular bone score; AGR: Albumin-to-globulin ratio; TyG: Triglycerides-glucose index; ALP: alkaline phosphatase; 25(OH)D: 25-hydroxivitamin D.